A New Induction Motor Drive Based on the Flux Vector Acceleration Method

Djordje Stojic, Slobodan Vukosavic, *Member, IEEE*

***Abstract*--A novel control strategy for the induction motor drive, based on the field acceleration method, is presented. The torque is controlled through variations of the stator flux angular velocity. The stator flux is controlled by using a feed-forward control scheme, with the stator flux reference vector adjusted so as to obtain the fixed rotor flux amplitude. The applied controller assures a fast torque response, low torque ripple in the steady state, and drive operation with a constant switching frequency. The algorithm includes the improved stator and rotor flux estimation that guarantees the stable drive operation in all operating conditions, even at low speeds. The experimental tests verify the performance of the proposed algorithm, proving that a good behavior of the drive is achieved in the transient and steady state operating conditions.**

***Index Terms*-- AC motor drives, flux vector estimation, sensorless torque control**

I. Introduction

THE induction motor drives with variable supply frequency are widely used in industry for the motion control, traction, and general automation. The effort in developing a novel control structures are focused on the drives having minimum number of sensors and measurement points required for the operation, monitoring, and drive protection. A wide range of speed-sensorless solutions has been proposed, resulting in a significant improvement of performance at higher speeds, but failing to improve the drive behavior below 1% of the rated speed.

The concept of Direct Torque Control (DTC) [1]-[2] improves the torque control performance and makes possible the elimination of local current controller. The use of the basic DTC concept with hysteresis controller [1]-[2] results in a very fast response unforeseen in conventional drives with a linear current controller in the minor loop. Yet, nonlinear hysteresis-based control results in an irregular inverter switching and a high value of the steady state ripple.

The torque chattering and switching frequency variations can be avoided by introducing IM drives with a fixed switching frequency [3]-[7]. Paper [3] presents an improved Direct Field-Oriented Vector Control (DFOC) algorithm, which includes an advanced method of rotor flux vector estimation by using an adaptive observer structure. To avoid the use of stator current controllers, the Stator Flux Vector Control (SFVC) [4]-[6] strategy, representing an extension of the DTC concept, is introduced. The aim of SFVC is to drive the stator flux vector towards the reference value through the Pulse Width Modulation (PWM) algorithm, with the reference stator flux calculated from the reference torque and reference rotor flux. As noted in [7], the advantage of SFVC compared to DFOC is that the SFVC has a faster torque dynamics, due to the absence of current controllers.

In [4], the SFVC drive with the predictive algorithm is presented, which enables the control of stator flux vector and torque values in the "dead-beat" fashion. Namely, the "dead-beat" control is achieved by calculating the appropriate voltage vector, which drives the flux and torque errors to zero in one sampling period. The predictive calculation of stator voltage vector requires the accurate values of IM model parameters, estimated flux vectors, and field velocity.

The SFVC algorithm [5] represents the linear stator flux controller, with the stator flux reference calculated from the rotor flux and the torque references; thus enabling the drive operation with constant rotor flux amplitude. Also, paper [5] introduces an improved stator and rotor flux estimation based on the closed-loop flux vector observer. The linear stator flux controller is designed in the feed-forward manner by introducing the stator resistance voltage drop and back-EMF feed-forward compensation. Namely, the feed-forward action consists of the stator flux multiplied by the feedback gain that varies proportionally to the field velocity. Finally, in [5], the torque control is based on the variation of the IM slip frequency.

In paper [6], the Decoupled Direct Control (DDC) of IM is presented, enabling the separate linear control of the torque and stator flux by using the decoupling matrix for the generation of stator voltage vector. The use of decoupling matrix enables independent controls of the torque and flux - the components of stator voltage vector are separately used - α and β components for the flux and torque, respectively. The paper [6] presents two DDC structures: the first based on the predictive control with the "dead-beat" fashion, and the second based on the PI control action, which is more robust than the first one regarding variations of IM parameters.

Papers [4]-[6] represent three different SFVC schemes, which prove that the direct linear control of torque and stator flux vector can assure a robust drive operation in relation to variations of motor parameters. Also, SFVC schemes enable a faster torque dynamics (response times t_r

Djordje Stojic is with the Electrical Institute INT, Golsvortijeva 13, 11000 Belgrade, Serbia & Montenegro (e-mail:djolestojic@yahoo.com)

Slobodan Vukosavic is with the Electrical Engineering Faculty, Belgrade, Bulevar Kralja Aleksandra 73, 11000 Belgrade, Serbia & Montenegro (e-mail:boban@ieee.org)

≈ 3 ms) compared to the DFOC algorithms. The shortcoming of the algorithms, which rely on the estimation of the flux vector velocity from the estimated stator flux vector, is the increased drive sensitivity in relation to the measurement noise and degradation of the drive performance caused by the flux estimation, especially at low speeds. Also, SFVC drives designed in the "dead-beat" fashion exhibit a high sensitivity with respect to IM parameter variations.

In order to overcome the aforementioned shortcoming of the existing algorithms, a novel SFVC algorithm is proposed in this paper. The introduced improvements result in a lower sensitivity to IM parameter variations and in an improved stability of drive operation, even at speeds close to zero. The performance improvement is achieved by the following changes of SFVC algorithm: by using the simplified feed-forward stator flux controller with a reduced set of control parameters, direct manipulation of the field velocity, and use of the closed-loop estimation of the stator and rotor fluxes.

The proposed solution is verified through a set of experimental tests on a setup using a 10-hp 4-pole industrial motor. The obtained results confirm that the proposed regulation strategy enables a stable drive operation in all practical working conditions, including the standstill.

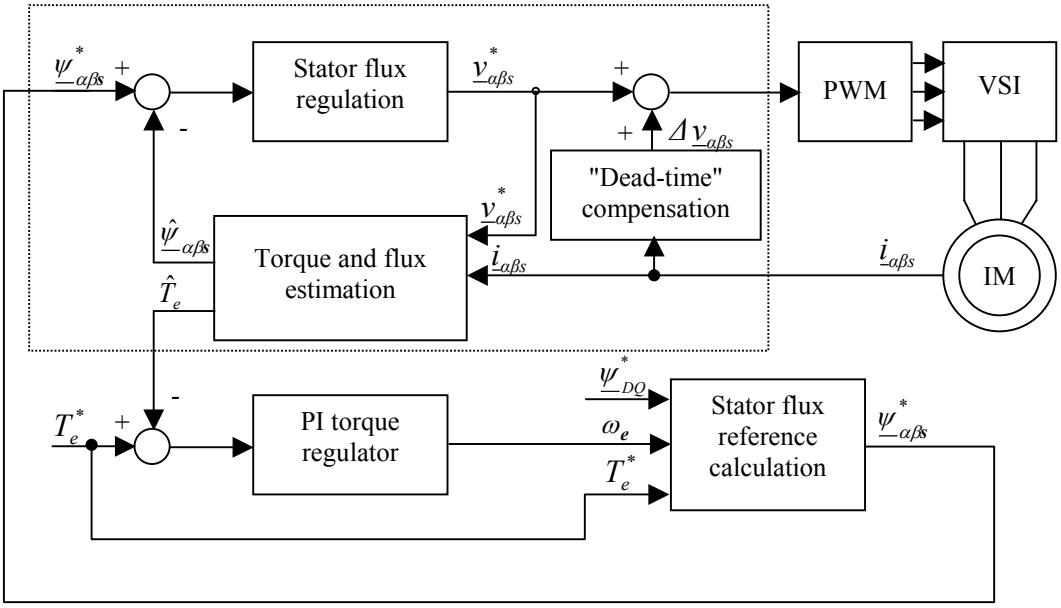

Fig. 1 Block diagram of SFVC algorithm

II. The Structure of the Proposed SFVC Drive

In the proposed SFVC algorithm, the torque control strategy relies on fundamental behavior of the squirrel cage induction motor - the torque proportional to the square of the rotor flux and the slip frequency, and inversely proportional to the rotor resistance. Hence, the torque control loop derives the torque error and increases/decreases the speed of field rotation. Consequently, the flux acceleration has impact on the slip frequency variations that will, in turn, result in a desired torque change and drive the torque error towards zero. The advantage of this approach to torque control is that the field rotation velocity is directly controlled, unlike the solutions in which the field velocity is calculated from the estimated stator flux vector and therefore is prone to the measurement noise and estimation distortions.

The proposed flux estimator and the flux controller are located in the stationary reference frame. The explicit flux control deals with the stator flux in order to achieve a faster response and to increase the robustness against parameter changes. The stator flux controller includes the feed-forward action, which requires the knowledge of only one IM parameter - stator resistance. On the other hand, the stator flux reference is calculated so as to take into account the component related to the leakage flux. In turn, the rotor flux amplitude is guaranteed to be constant in a constant-torque operating mode, simplifying the torque control by making the slip-torque relation linear. By operating in the constant-torque mode, the proposed solution ensures a low torque ripple and a constant switching frequency. The algorithm requires a relatively small number of the torque and flux controllers parameters to be set, and has the simplicity of implementation, parameter setting, and use.

Fig. 1 shows the block diagram of the proposed drive. The main outer loop represents the torque controller, which determines the value of flux velocity ω_e, i.e., the velocity of the reference vector $\underline{\psi}^*_{\alpha\beta s}$. The value of synchronous velocity ω_e is determined by the torque PI controller, in the main control loop. The direct manipulation of ω_e, performed by the torque controller, improves the drive stability. The amplitude of stator flux reference $\underline{\psi}^*_{\alpha\beta s}$ is calculated from the rotor flux and torque references, in order to enable a constant rotor flux amplitude at the constant-torque operating mode.

The minor inner loop, inside the dotted rectangle in Fig. 1, represents the linear stator flux controller. The flux controller is realized in the stationary reference frame with the zero stator flux error, in the steady state. It produces the reference stator voltage vector $\underline{v}^*_{\alpha\beta s}$, to be fed into the PWM

block. The stator flux controller has a simplified feed-forward structure. Namely, the feed-forward compensation of the back-EMF is proportional to the stator flux reference vector $\underline{\psi}^*_{\alpha\beta s}$, unlike [5] with the feed-forward action proportional to the estimated stator flux vector. In such way, the stability of drive is improved, especially at low speeds.

The flux controller in Fig.1 includes the block of the flux vector calculation. The problems associated with the flux estimation are resolved by using the stator flux observer, based on the closed-loop estimation with the rotor flux used as the feedback signal. The use of the closed-loop observer introduces a significant improvement in the behavior of the drive. The closed-loop flux observer also resolves the problems related to the dc-drift of estimator output.

III. The Estimation of the Stator Flux Vector

The flux vector estimation uses the stator current and stator voltage as input variables. The stator currents are measured by using the current probes. The stator voltage vector can be directly measured at the motor terminals. This solution requires the electrical insulation between the power circuit and control hardware. On the other hand, the voltage reference values can be used instead of the voltage measurements. When using the reference voltage value instead of the measured data, the difference between the two should be considered. This difference is caused by the inverter nonlinearities [8]. If not compensated, these effects are manifested especially at near-zero speeds when the voltage fundamental is low.

In order to avoid the use of expensive measurement hardware, we use the voltage reference vector $\underline{v}^*_{\alpha\beta s}$ for the flux vector estimation. In addition, to avoid the irregular drive operation at low speeds, the VSI "dead-time" effect is compensated by using the algorithm proposed in [9].

The problems associated with the flux estimation are resolved by using the flux observer based on a closed-loop estimation scheme [5], [10], [11]. Such flux estimation is developed from the general *dq* rotational frame model of IM expressed by the following equations

$$\underline{v}_{dqs} = \underline{i}_{dqs} R_s + j\omega \underline{\psi}_{dqs} + \frac{d\underline{\psi}_{dqs}}{dt} \tag{1}$$

$$0 = \underline{i}_{DQ} R_r + j(\omega - \omega_r)\underline{\psi}_{DQ} + \frac{d\underline{\psi}_{DQ}}{dt} \tag{2}$$

$$\underline{\psi}_{dqs} = L_s \underline{i}_{dqs} + M \underline{i}_{DQ} \tag{3}$$

$$\underline{\psi}_{DQ} = L_r \underline{i}_{DQ} + M \underline{i}_{dqs} \tag{4}$$

$$T = \frac{3}{2} p\left(\psi_{ds} i_{qs} - \psi_{qs} i_{ds}\right) \tag{5}$$

where p is the number of pole pairs, ω is the reference frame angular velocity, ω_r is the rotor speed, v_{dqs} is the stator voltage vector, i_{dqs} is the stator current vector, i_{DQ} is the rotor current vector, ψ_{dqs} is the stator flux vector, ψ_{DQ} is the rotor flux vector, R_s is the stator resistance, R_r is the rotor resistance, L_s is the stator inductance, L_r is the rotor inductance, M is the mutual inductance, while j represents the imaginary unit. For the stationary $\alpha\beta$ reference frame, equations (1)-(5) are modified by setting $\omega = 0$.

The stator flux can be determined by solving differential equation (1). This type of flux estimation introduces a positive current feedback in the control loop, thus causing the unstable drive operation at low speeds. This instabilities originate from the inaccurate value of stator resistance in (1) and from effects of inverter nonlinearities amplified by the stator current feedback.

The flux estimation can be improved by introducing a negative current feedback in the flux vector calculation. This feedback is introduced by using the closed-loop flux observer. The operating principle of the closed-loop flux estimator is based on feeding back the difference between the reference and estimated rotor flux vector. The difference signal is used to correct the voltage model (1), thus minimizing the error of flux estimation. The difference signal also includes the negative feedback path for the stator current, canceling out the negative influence of the flux estimator on the stability of drive operation. The behavior of flux estimator is governed by the following equations

$$\hat{\underline{\psi}}_{\alpha\beta s} = \int [\underline{v}_{\alpha\beta s} - R_s \underline{i}_{\alpha\beta s} + G(\underline{\psi}^*_{\alpha\beta r} - \hat{\underline{\psi}}_{\alpha\beta r})]\, dt \tag{6}$$

$$\hat{\underline{\psi}}_{\alpha\beta r} = \frac{L_r}{M} \hat{\underline{\psi}}_{\alpha\beta s} - \frac{\sigma L_s L_r}{M} \underline{i}_{\alpha\beta s} \tag{7}$$

where $\underline{\psi}^*_{\alpha\beta r}$ represents the rotor flux reference vector and G is the observer gain. Vector $\underline{\psi}^*_{\alpha\beta r}$ is calculated from rotor flux reference vector $\underline{\psi}^*_{DQ}$ by using the inverse rotational transformation from the *dq* frame, synchronous with vector $\underline{\psi}^*_{DQ}$. The observer gain G is chosen according to the criterion that the stable drive operation is to be maintained for variations of R_s within 25%. The value of G is chosen experimentally, on the setup with detuned value of $R_s \pm 25\%$ used in the algorithm. For the detuned parameter R_s, the stable drive operation is obtained by increasing G. The adopted value of G is given in Appendix.

Equation (7) is used to calculate the estimated value of rotor flux vector by using stator flux vector estimates (6) and measured samples of stator current. The estimated rotor flux value (7) is used as the feedback signal in the closed-loop stator flux observer (6). The flux observer enables the stable drive operation, even at very low speeds. It is also less sensitive to variations of drive parameters and to the nonlinearities of the voltage inverter. The performance of the proposed observer is comparable to more complex and more time-consuming solutions based on the full-order observers and Kalman filter.

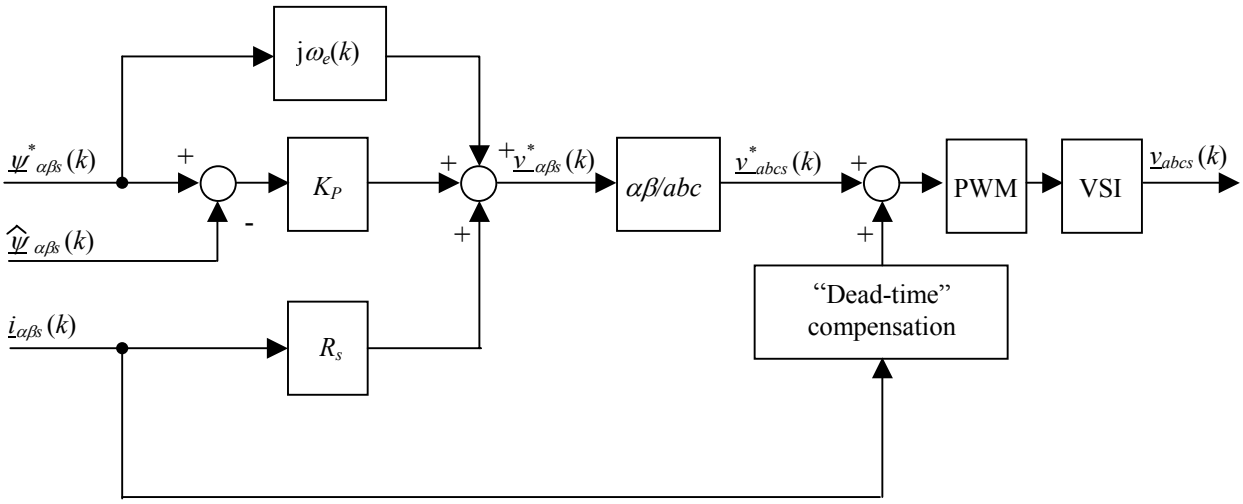

Fig. 2 Block diagram of stator flux regulator

IV. The Stator Flux Controller

The stator flux controller determines the value of voltage reference in the stationary reference frame. The voltage value is calculated in order to obtain the stator flux equal to the reference vector $\underline{\psi}^*_{\alpha\beta s}$ in the finite settling time. The control is designed to achieve the zero flux error in less then three sampling periods. The settling time is $t_{st} = (2\text{-}3)T_s$, where T_s denotes the sampling period $T_s = 200\ \mu$s of the digital controller.

Since the flux controller is designed in the stationary $\alpha\beta$ reference frame, with the sinusoidal and variable-frequency references, it is necessary to design the control structure that guarantees zero stator flux error signals in the steady state. To this end, the zero error signal in the steady state is obtained by implementing the feed-forward control structure. Fig. 2 shows the stator flux controller, together with the space vector pulse width modulator and "dead-time" compensation.

The flux controller is given by

$$\underline{v}^*_{\alpha\beta s}(k) = R_s \underline{i}_s(k) + j\omega_e(k)\underline{\psi}^*_{\alpha\beta s}(k) + K_P[\underline{\psi}^*_{\alpha\beta s}(k) - \underline{\hat{\psi}}_{\alpha\beta s}(k)]. \quad (8)$$

The first two terms on the right hand side of (8) represent the feed-forward control actions aimed at compensating the voltage drop on the stator resistance and stator back-EMF. This actions determine the steady state stator voltage that guarantees the zero stator flux error, for the stator flux reference vector $\underline{\psi}^*_{\alpha\beta s}$. The third term on the right hand side of (8) represents the feedback control action proportional to the stator flux error. In (8), K_P denotes the gain of the flux controller and $\omega_e(k)$ represents the instantaneous stator flux velocity determined by the outer torque control loop. Since the increase of K_P produces a faster response of the stator flux, K_P may be tuned experimentally by increasing K_P until a stable transient response with the settling time equal to $t_{st} = 3T_s$ is achieved. The adopted value of K_P is given in Appendix.

The proposed control strategy (8) includes the feed-forward action proportional to the stator flux reference vector. This is an improvement compared to the solutions that include the feed-forward action proportional to the estimated stator flux vector, in which variations of field velocity introduce changes of the drive dynamic characteristics. These variations are advantageously avoided by using the structure proposed in (8).

The feed-forward term in (8), used to compensate the voltage drop on the stator resistance, exists in various SFVC schemes [4], [5]. This feed-forward action represents the positive feedback path for the stator current. Consequently, it increases the sensitivity of the drive in relation to the nonlinearities of VSI and to variations of R_s. The stability problems related to the intrinsic positive current feedback, introduced by the feed-forward action, are resolved by using the closed-loop stator flux estimator. Namely, such flux estimation introduces a negative feedback path for the stator current that improves the drive stability and lowers the sensitivity of the drive in relation to the VSI nonlinearities and parameter variations.

Along with the stator flux controller structure, the algorithm for the stator flux reference calculation is defined. The algorithm for calculation of the stator flux reference vector $\underline{\psi}^*_{\alpha\beta s}$ ensures the drive operation with constant rotor flux amplitude. Namely, by using the rotational reference frame model of IM (1)-(5), under condition of the constant rotor flux amplitude, the stator currents can be calculated from the electromagnetic torque. Hence, for the rotor flux references $\psi^*_Q = 0$, $\psi^*_D = \mathrm{C}$, and for the torque reference T^*_e, the reference stator currents are determined by

$$i^*_{qs} = \frac{2\ L_r}{3\ p\ M\ \psi^*_D} T^*_e \quad (9)$$

$$i^*_{ds} = \frac{\psi^*_D}{M}\ . \quad (10)$$

From equations (7), (9), and (10), the stator flux reference vector is calculated as

$$\underline{\psi}^*_{\alpha\beta s} = \frac{M}{L_r}\underline{\psi}^*_{\alpha\beta r} + \sigma\ L_s \underline{i}^*_{\alpha\beta s} \quad (11)$$

where vectors $i^*_{\alpha\beta s}$ and $\psi^*_{\alpha\beta r}$ are calculated from vectors i^*_{dqs} and ψ^*_{DQ}, respectively, by using the inverse rotational transformation from the rotational reference frame synchronous with the rotor flux reference vector.

Together with the calculation of $v^*_{\alpha\beta s}(k)$, the stator flux controller includes the "dead-time" compensation achieved

by using the algorithm proposed in [9]. The compensation is based on calculation of volt seconds lost in the blanking period averaged over the switching cycle. Since the voltage distortion introduced by the blanking time is of the opposite sign to the phase currents, the compensation voltage component Δv_s is added to the commanded voltage $\underline{v}^*_{abcs}$ with the same sign as the appropriate phase current. The "dead-time" compensation is expressed as

$$\underline{v}_{abcs} = \underline{v}^*_{abcs} + \Delta v_s \operatorname{sign}\left(\underline{i}_{abcs}\right). \tag{12}$$

V. The Torque Regulation

In the previous section, it has been shown that the control of stator flux may be performed for all drive operating frequencies. The stator flux control is extended to the torque control by introduction of the linear torque regulation, through manipulation of the value of field velocity.

By using the model of IM in the generalized rotational frame (1)-(5), the following equation is derived

$$T_e = \frac{3}{2}\frac{p\left|\underline{\psi}_{\alpha\beta r}\right|^2}{R_r}\omega_{sl} \tag{13}$$

showing that the steady state slip frequency determines the steady state torque value.

The change in the slip frequency yields an instantaneous change of torque [1] (the increase of slip velocity causes the torque increase, and vice versa). Since the slip frequency ω_{sl} represents the difference between the field velocity ω_e and rotor speed ω_r ($\omega_{sl} = \omega_e - \omega_r$), the torque can directly be controlled by variations of ω_e, due to the fact that the rotor speed represents a slowly varying variable compared to the torque. The instantaneous angle of the rotor flux reference $\underline{\psi}^*_{\alpha\beta r}$ is calculated by integrating ω_e.

Since the steady state field velocity of IM depends on the reference torque and rotor speed values, the appropriate algorithm for calculation of ω_e is selected in order to enable the zero torque error in all operating conditions. In several SVFC algorithms, the field velocity is calculated from IM model by using the estimated stator flux vector. This approach is sensitive to the measurement noise and nonlinearities of VSI. Therefore, the different method for calculation of ω_e is applied. Namely, the torque error is fed in the PI controller, while the controller output is used as the value for synchronous velocity ω_e. The applied torque controller creates both the transient and steady state components of the synchronous velocity ω_e, thus enabling the fast torque response and zero torque error in the steady state. The employed linear torque controller also enables the minimum torque ripple in the steady state, with the constant switching frequency operation.

The PI torque controller is defined by the following equation

$$\omega_e(k) = \omega_e(k-1) + K_{T1}[\Delta \hat{T}_e(k) - K_{T2}\,\Delta \hat{T}_e(k-1)] \tag{14}$$

where K_{T1} and K_{T2} are the controller parameters, and $\Delta \hat{T}_e(k)$ represents the torque error ($\Delta \hat{T}_e(k) = T_e^*(k) - \hat{T}_e(k)$). The torque controller operates with the sampling period of 200 μs. The torque controller parameters K_{T1} and K_{T2} are determined experimentally by using the standard procedure proposed in [12]. In doing so, the speed of response of the main torque control loop three times slower compared to the speed of response of the minor flux control loop should be obtained. Since the settling time of the flux controller is (2-3)T_s, the settling time of torque controller is less than $9T_s$. The calculated values of K_{T1} and K_{T2} are given in Appendix.

The performance of the torque controller is verified through the set of experimental tests presented in the following section.

VI. The Experimental Results

The setup comprises the three phase VSI with IGBTs. The stator voltage commands are modulated by using symmetrical PWM, constant switching frequency f_{PWM} = 5 kHz, and lockout time 4±0.5 μs. The DC bus voltage of the VSI is 540±20 V, with the VSI over-current protection set to 100 A. The PWM modulation and stator currents sampling are realized by using a custom FPGA based hardware, with measurement executed by using the 12-bit resolution. The stator current signals are, prior to A/D conversion, filtered by using a first-order anti-aliasing filters having the bandwidth set to 30 kHz. The currents are sampled at the instances in the middle of the symmetric PWM cycle, in order to minimize the ripple component in the stator current measurements. The sampling period is set to T_s = 200 μs, with the flux estimator, flux and torque regulator having the same sampling time. The flux estimation, flux and torque control algorithms are implemented on a PC platform, running the real-time control software with the floating-point arithmetic precision.

The induction machine under test was coupled to a separately controlled DC machine used as a dynamic brake. The 4-pole squirrel cage induction motor is characterized by the data given in Appendix.

The steady state and transient behavior of the drive was investigated through various sets of experimental tests.

A. The steady state operating conditions of the torque controller

The investigation of drive behaviour in the steady state is necessary in order to determine the following drive characteristics: the stability of drive operation, torque ripple in the steady state, and torque steady-state error. The investigation of these characteristics enables the comparison of the outlined strategy with the existing DTC strategies. The steady state behaviour is investigated in the different operating conditions, e.g., with the locked rotor, for the mid- and high-speed regions.

The drive behaviour in operating conditions with low synchronous frequencies was examined by using the locked rotor tests. These tests are of the special interest, since the stability of the basic DTC strategies [1]-[2] is undermined in these operating conditions.

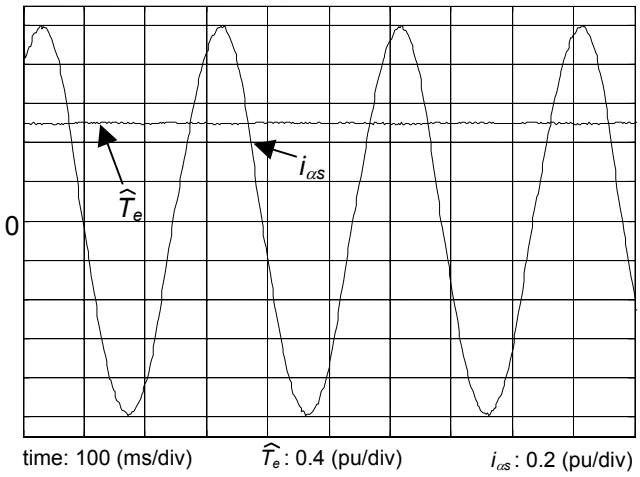

Fig. 3. Estimated torque and stator current for the locked rotor and nominal torque

Fig. 3 shows the current and torque behaviors for the locked rotor with the rotor flux and torque set to their rated values. Since the rotor is locked, the drive operates in the range of very low field rotation frequencies. Generally, the sensorless IM control strategies exibit the deterioration of operation performance at low field frequencies. In this case, the voltage fundamental is very small and comparable with the level of voltage distorsions exibited by VSI, which may cause the poor flux estimation and instabilities of drive operation. The traces presented in Fig. 3 prove that the drive operation is stable, without nonlinear distorsions of the stator current. Also, the torque steady-state error is zero, while the torque ripple is bellow 5%, which is an improvement when compared to the basic DTC strategies with the torque ripple above 20%. The experimental results in Fig. 3 prove that the proposed PI torque control algorithm enables the zero torque-error signal in the standstill. This proves that the precise and stable torque regulation can be achieved with the PI control strategy, unlike the existing SFVC algorithms that achieve less stable drive operation in the low speed region by using more complex control strategies.

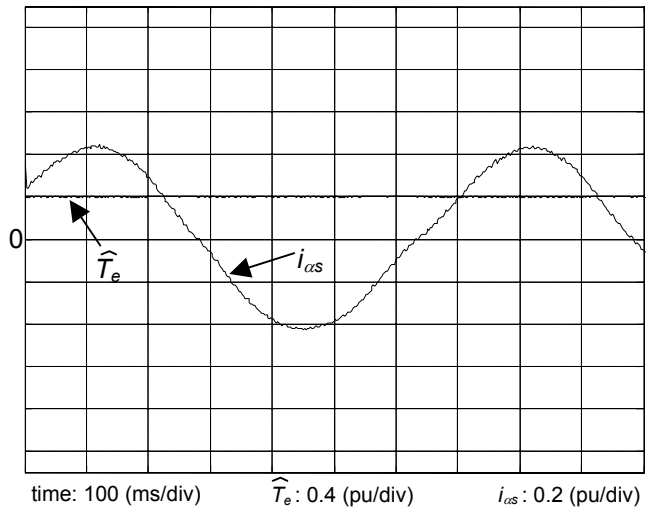

Fig. 4. Estimated torque and stator current for the locked rotor and torque set to 0.4 pu

Fig. 4 shows the test results for torque reference set to 0.4 pu. In this experiment, the drive operates with even lower field velocity than in the previous test. The presented experimental results prove that, for near-zero values of ω_e, the drive retains stability and operates accurately with a low distortion of the stator current.

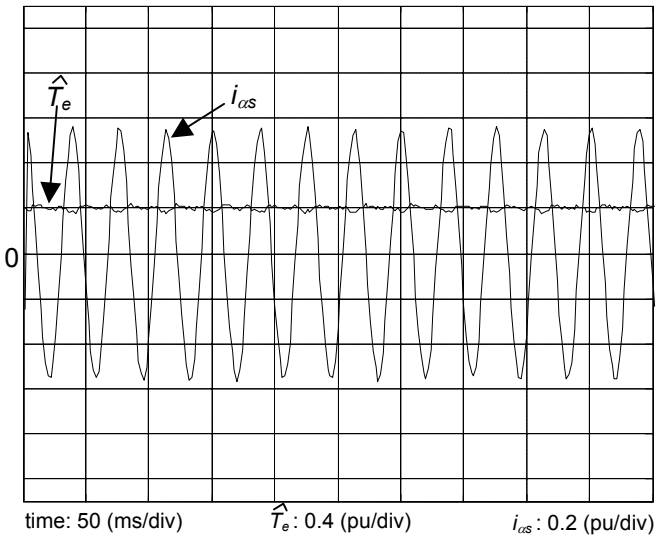

Fig. 5. Estimated torque and stator current for the speed set to 0.5 pu and torque set to 0.4 pu

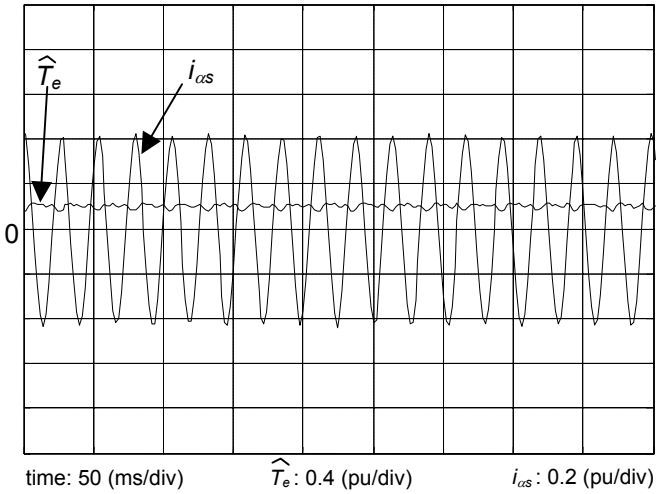

Fig. 6. Estimated torque and stator current for the speed set to 0.8 pu and torque set to 0.2 pu

Fig. 5 presents the results for the mid-speed region with the torque set to 0.4 pu, and rotor speed set to 0.5 pu by DC motor coupled with IM. Fig. 6 shows the torque and stator current behaviours for the torque set to 0.2 pu and speed set to 0.8 pu. The experimental results in Figs. 5 and 6 prove that, in the mid- and high-speed region, the stator current is sinusoidal with small distorsions, while the torque matches its reference value. The presented results also prove that the drive operates stably and accurately in the steady state within a wide range of rotor speeds.

Results presented in this subsection show that the proposed PI torque control technique enables the zero torque-error operation in the stationary-state within a wide range of operating speeds. This is an improvement compared to "dead-beat" SFVC solutions, which require the accurate knowledge of the full set of motor parameters to generate adequate command values for the zero torque-error operation in variable drive operating conditions.

B. The transient operating conditions of the torque controller

The transient behaviour of the proposed DTC algorithm was investigated for the locked rotor, low- and mid-speed regions. The transient experimental tests are necessary to investigate the dynamics of the torque controller.

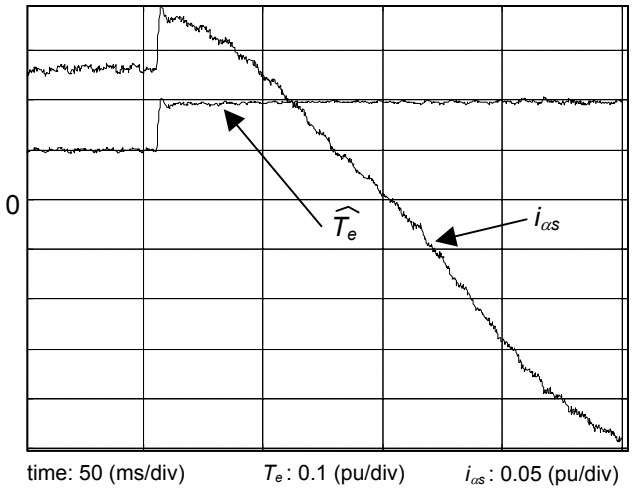

Fig. 7. Torque and stator current responses for the locked rotor and torque reference step excitation from 0.1 to 0.2 pu

Fig. 7 shows torque and stator current responses for the locked rotor and torque reference step change from 0.1 to 0.2 pu. The presented results show that the response time of torque, for the step excitation, is equal to 4-5 sampling periods (T_s = 200 μs), while the settling time is (9-10)T_s with the zero steady-state error. This test shows that the proposed DTC algorithm has a response times comparable to those achieved with the basic DTC algorithms. Moreover, even though the basic DTC strategies exhibit the response times of 1-2 sampling periods, they can hardly meet requirements for the stable operation and law torque ripple in all operating conditions. Also, the presented results prove that the achieved speed of torque response is faster compared to existing SFVC strategies.

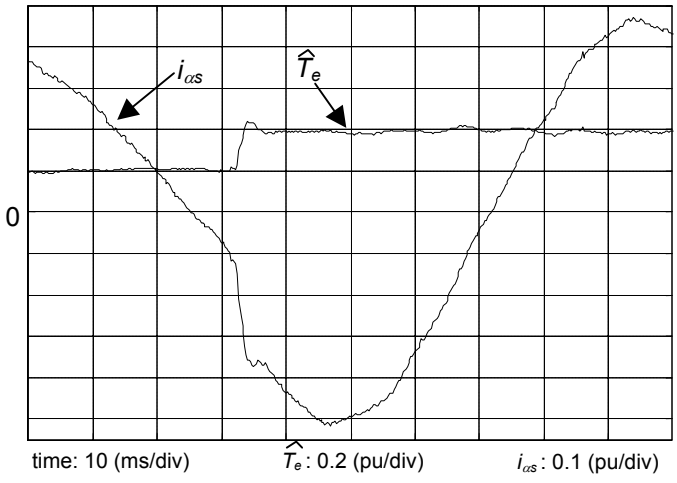

Fig. 8. Torque and stator current responses for the speed set to 0.2 pu and torque reference step excitation from 0.2 to 0.4 pu

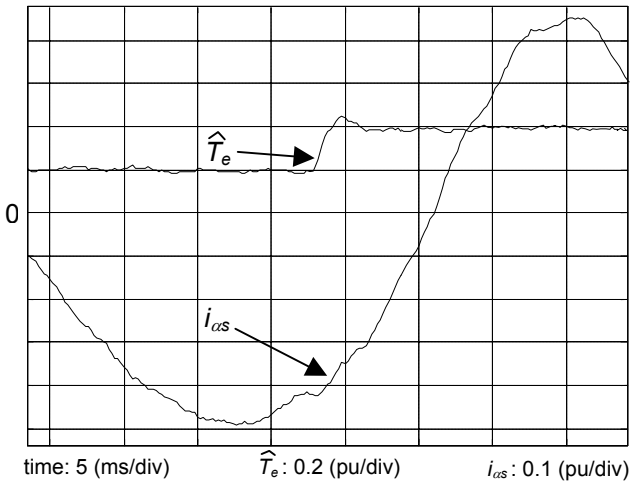

Fig. 9. Torque and stator current responses for speed set to 0.4 pu and for torque reference step excitation from 0.2 to 0.4 pu

Fig. 8 shows the torque response on the step excitation from 0.2 to 0.4 pu, for the rotor speed set to 0.2 pu. Also, the traces of Fig. 9 represent the torque response on the step excitation, for the rotor speed set to 0.4 pu. The presented test results prove that the proposed SFVC algorithm is robust in relation to rotor speed variations, i.e., it retains approximately the same dynamic characteristics in a wide range of operating speeds.

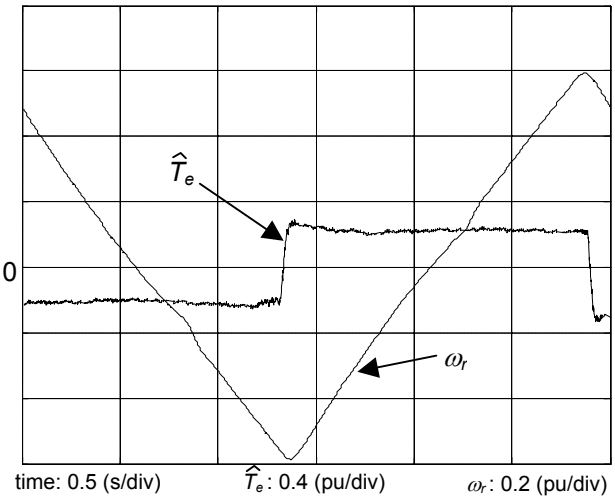

Fig. 10. Estimated torque and actual rotor speed for torque reversal

The traces of Fig. 10 represent the rotor speed behaviour for the torque reversal, showing that the rotor speed has a typical "saw-tooth" waveform, without significant distortions of the speed waveform. This experiment is performed in order to enable further comparison of the proposed algorithm with the existing SFVC drives. Namely, the torque and speed measurements in Fig. 10 prove that the stability of the drive in the low-speed is improved, since the existing SFVC drives exhibit higher speed and torque distortions in the near-zero speed operation. This proves that in the proposed algorithm the estimated torque value matches the real torque value to a greater extent compared to the existing SFVC drives, in a wide range of operating conditions.

VII. Conclusion

A novel DTC algorithm has been presented, based on the SFVC of an induction motor. The algorithm requires the relatively small number of parameters to be set and has the simplicity of implementation. The torque controller manipulates the velocity of the field rotation, to drive the torque error towards zero and to enable the drive operation with constant switching frequency and a minimum torque ripple. The flux control deals with the stator flux to achieve a faster response and to increase the robustness against IM parameter changes. The stator flux reference is calculated so as to keep the rotor flux amplitude constant, enabling the control by making the slip-torque relation linear. The stator and rotor fluxes are estimated by using the closed-loop observer, thus improving the stability of operation and reducing the sensitivity of the drive against parameter variations and nonlinearities of VSI.

The proposed solution is verified on an experimental setup having 10-hp, 4-pole standard induction motor. The obtained results confirm the ability of the proposed controller to enable the torque and speed control in all operating conditions, including the standstill.

VIII. Appendix

The parameters of the induction machine: P = 7.5 kW, n=1500 rpm, V = 220 V, f = 50 Hz, R_s= 2.1 Ω, R_r=1.2 Ω, L_s= 52 mH, L_r = 52 mH, L_m = 50 mH.

The control parameters: K_p = 300, G = 200, K_{T1}= 1.5, K_{T2} = 0.95.

IX. References

[1] I. Takahashi, T. Noguchi, “A new quick-response and high-efficiency control strategy of an induction motor," *IEEE Trans. on Industrial Applications,* vol. 22, pp. 820-827, Sept/Oct. 1986.

[2] M. Depenbrok. “Direct self-control (DSC) of inverter-fed induction machine,” *IEEE Trans. on Power Electronics, v*ol. 3, pp. 420-429, October 1988.

[3] K. Matsuse*,* Y. Kouno, H. Kawai, and S. Yokomizo, "A speed-sensorless vector control method of parallel-connected dual induction motor fed by a single inverter," *IEEE Trans. on Industry Applications*, vol. 38, pp. 1566-1571, November/December 2002.

[4] J. Lee, C. Kim, M. Youn, "A dead-beat type digital controller for the direct torque control of an induction motor," *IEEE Trans. on Power Electronics,* vol. 17, pp. 739-746, September 2002.

[5] D. Casadei, G. Serra, A. Tani, L. Zarri, F. Profumo “Performance analysis of a speed-sensorless induction motor drive based on a constant switching frequency DTC scheme,” *IEEE Trans. on Industry Applications*, vol. 39, pp.476-483, March/April 2003.

[6] C.Moucary, E.Mendes*,* A.Razek*,* "Decoupled direct control for PWM inverter-fed induction motor drives," *IEEE Trans. on Industry Applications*, vol. 38, pp.1307-1315, September/October 2002.

[7] D. Casadei, F. Profumo, G. Serra, A. Tani, "FOC and DTC: two viable schemes for induction motors torque control," *IEEE Trans. on Industry Applications*, vol. 17, pp 779-787, September 2002.

[8] J. Holtz, J. Quan, "Sensorless vector control of induction motors at very low speed using a nonlinear inverter model and parameter identification," *IEEE Trans. on Industry Applications*, vol. 38, pp.1087-1095, July/August 2002.

[9] J.W. Choi and S.K. Sul, “Inverter output voltage synthesis using novel dead time compensation,” *IEEE Trans. Power Electron*., vol. 11, pp.221–224, Mar. 1996.

[10] J. Holtz, "Drift and parameter compensated flux estimator for persistent zero stator frequency operation of sensorless controlled induction motors," in *Proc. IEEE-IAS 2002, 37th Annual IAS Meetin*g, vol. 3, pp. 1687-1694

[11] M. Hinkkanen and J. Luomi, "Parameter sensitivity of full-order flux observers for induction motors", in *Proc. IEEE-IAS 2002, 37th Annual IAS Meeting*, vol. 2, pp. 851-855

[12] K.J. Astrom and T. Hagglund, *PID Controllers:Theory, Design, and Tuning,* Instrument Society of America, pp. 136-138, 1995.

Djordje M. Stojic was born in Belgrade, Serbia, Yugoslavia, in 1970. He received the B.S., and M.S. degrees from the Electrical Engineering Faculty, University of Belgrade, Belgrade, Yugoslavia, in 1994, and 1996, respectively. He is currently pursuing Ph.D. degree at the Electrical Engineering Faculty, University of Belgrade.

Currently he is employed at the Nikola Tesla Institute, Belgade, Yugoslavia as a Develompent Engineer in the area of microcomputer-based industrial control. His research interests include analysis and development of electric drives.

Slobodan N. Vukosavic (M’93) was born in Sarajevo, Bosnia and Hercegovina, Yugoslavia, in 1962, He received the B.S., M.S., and Ph.D. degrees from the Electrical Engineering Faculty, University of Belgrade, Belgrade, Yugoslavia, in 1985, 1987, and 1989, respectively.

He conducted research in the areas of static power converters and microcomputer-based control of electrical drives the Nikola Tesla Institute, Belgrade, Yugoslavia, until 1988, when he joined the ESCD Laboratory of Emerson Electric, St. Louis, MO, in the co-operative appliance drive research program, In 1991, he joined Vickers Company, Milan, Italy, as a Project Leader. He returned to Belgrade University in 1995, where he is currently an Associate Professor. His scientific interests are in the areas of electromechanical conversion, modeling, and identification, DSP-based power conversion control, and power electronics. He has published numerous articles, several student textbooks, and a number of invited papers.